KDM6 demethylases integrate DNA repair gene regulation and loss of KDM6A sensitizes human acute myeloid leukemia to PARP and BCL2 inhibition

Liberalis Debraj Boila
Indian Institute of Chemical Biology
Subhadeep Ghosh
Indian Institute of Chemical Biology
Subham Bandyopadhyay
Indian Institute of Chemical Biology
Liqing Lin
Princess Margaret Cancer Centre, University Health Network
Alexander Murison
Princess Margaret Cancer Centre, University Health Network
Andy Zeng
Princess Margaret Cancer Centre
Wasim Shaikh
Indian Institute of Chemical Biology
Satyaki Bhowmik
Indian Institute of Chemical Biology
Siva Sai Naga Anurag Muddineni
Tel Aviv University
Mayukh Biswas
Indian Institute of Chemical Biology
Sayantani Sinha
Indian Institute of Chemical Biology
Shankha Subhra Chatterjee
Indian Institute of Chemical Biology
Nathan Mbong
Princess Margaret Cancer Center
Olga Gan
Princess Margaret Cancer Center
Anwesha Bose
Indian Institute of Chemical Biology

Sayan Chakraborty
Indian Institute of Chemical Biology
Andrea Arruda
Princess Margaret Cancer Centre
James Kennedy
Princess Margaret Cancer Centre
Amanda Mitchell
Princess Margaret Cancer Centre
Eric Lechman
Princess Margaret Cancer Centre
Debasis Banerjee
R K Mission Seva Pratisthan & Hospital
Michael Milyavsky
Tel Aviv University https://orcid.org/0000-0002-5083-0809
Mark Minden
University Health Network
John Dick
Princess Margaret Cancer Centre - the University Health Network
Amitava Sengupta (amitava.iicb@gmail.com)
Indian Institute of Chemical Biology

Article

Keywords: AML, KDM6, PARP, BCL2, Combination targeted therapy

Posted Date: September 27th, 2022

DOI: https://doi.org/10.21203/rs.3.rs-2064697/v1

Graphical abstract

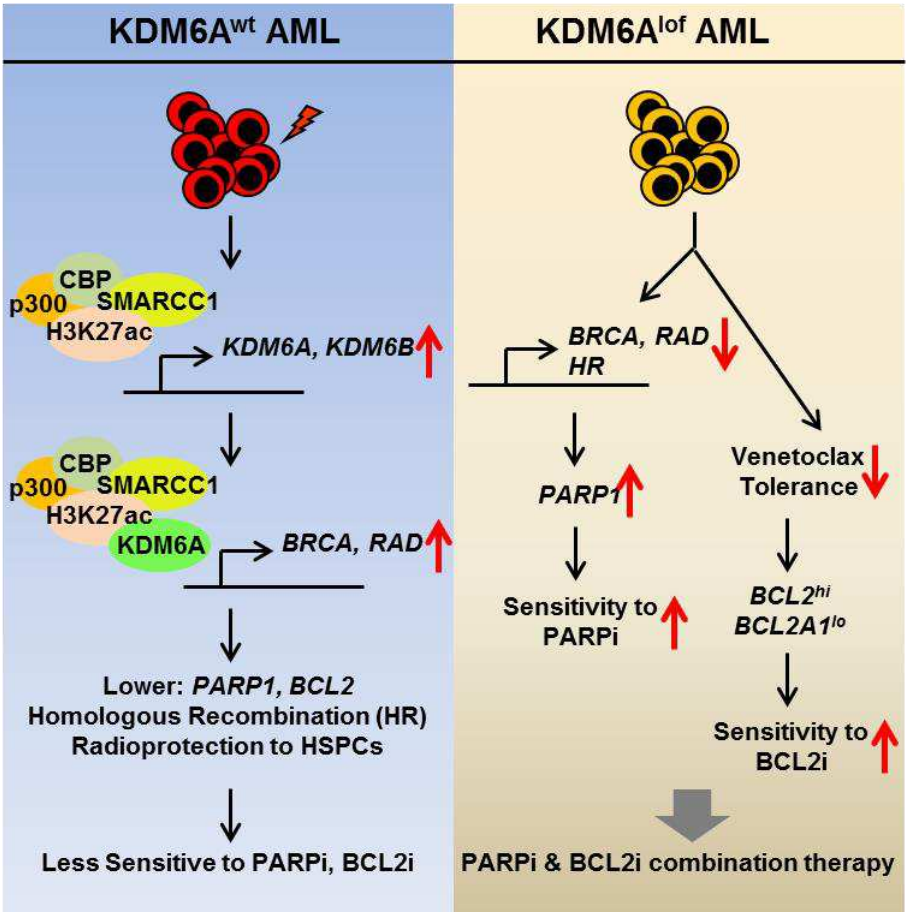

ARTICLE

KDM6 demethylases integrate DNA repair gene regulation and loss of KDM6A sensitizes human acute myeloid leukemia to PARP and BCL2 inhibition

Liberalis Debraj Boila[1, #], Subhadeep Ghosh[1, 2, #], Subham K. Bandyopadhyay[1, 2, #], Liqing Jin[3], Alex Murison[3], Andy G. X. Zeng[3, 4], Wasim Shaikh[1, 2], Satyaki Bhowmik[1, 2], Siva Sai Naga Anurag Muddineni[5], Mayukh Biswas[1], Sayantani Sinha[1], Shankha Subhra Chatterjee[1], Nathan Mbong[3], Olga I. Gan[3], Anwesha Bose[1, 2], Sayan Chakraborty[1], Andrea Arruda[3], James A. Kennedy[3, 6, 7], Amanda Mitchell[3], Eric R. Lechman[3], Debasis Banerjee[8], Michael Milyavsky[5], Mark D. Minden[3, 6, 7, 9], John E. Dick[3, 4, *] and Amitava Sengupta[1, 2, 10, *]

[1]Stem Cell & Leukemia Lab, CSIR-Indian Institute of Chemical Biology, IICB-Translational Research Unit of Excellence, Salt Lake, Kolkata 700091, West Bengal, India
[2]Academy of Scientific & Innovative Research (AcSIR), CSIR-Indian Institute of Chemical Biology, 4, Raja S.C. Mullick Road, Jadavpur, Kolkata 700032, West Bengal, India
[3]Princess Margaret Cancer Centre, University Health Network, Toronto, ON, M5G 1L7, Canada
[4]Department of Molecular Genetics, University of Toronto, Toronto, ON, M5S 1A8, Canada
[5]Department of Pathology, Sackler Faculty of Medicine, Tel Aviv University, Israel 6997801
[6]Division of Medical Oncology and Hematology, Department of Medicine, University Health Network, Toronto, ON, M5G 2C4, Canada
[7]Department of Medicine, University of Toronto, Toronto, ON, M5S 1A8, Canada
[8]Park Clinic, Gorky Terrace and Ramakrishna Mission Seva Pratisthan, Kolkata 700017, West Bengal, India
[9]Department of Medical Biophysics, University of Toronto, Toronto, ON, M5G 1L7, Canada
[10]CSIR-IICB-Cancer Biology & Inflammatory Disorder Division, 4, Raja S.C. Mullick Road, Jadavpur, Kolkata 700032, West Bengal, India

Present Address: L.D.B. Human Biology Division, Fred Hutchinson Cancer Research Center, Seattle, WA 98109, USA; M. B. Irving Cancer Research Center, Columbia University Medical Center, New York, NY, 10032, USA; S.S. Clinical Research Division, Fred Hutchinson Cancer Research Center, Seattle, WA 98109, USA; S.S.C. Department of Pathology and Laboratory Medicine, Weill Cornell Medicine, New York, NY 10065, USA

Running Title: KDM6A determines PARP and BCL2 blockade in AML
Keywords: AML; KDM6; PARP; BCL2; Combination targeted therapy

*Correspondence: Lead Contact: Amitava Sengupta, CSIR-Indian Institute of Chemical Biology, CN-6, Sector V, Salt Lake, Kolkata 700091, West Bengal, India; Email: amitava.sengupta@iicb.res.in; Ph: +91 33-2340-3000
John E. Dick, Princess Margaret Cancer Centre, 101 College Street, PMCRT, Toronto, M5G 1L7, ON, Canada; Email: john.dick@uhnresearch.ca; Ph: +1 416-581-7472

[#]L.D.B., S.G., and S.K.B. contributed equally. S.G., and S.K.B. can be interchangeably made co-first authors

Number of Figures: 7, Supplemental Figures: 8, Supplemental Tables: 3, Supplemental Datasets: 4

ABSTRACT

Acute myeloid leukemia (AML) is a heterogeneous, aggressive malignancy with dismal prognosis and with limited availability of targeted therapies. Epigenetic deregulation contributes to AML pathogenesis. KDM6 proteins are histone-3-lysine-27-demethylases that play context-dependent roles in AML. We inform that KDM6-demethylase function critically regulates DNA-damage-repair-(DDR) gene expression in AML. Mechanistically, KDM6 expression is regulated by genotoxic stress, with deficiency of KDM6A-(UTX) and KDM6B-(JMJD3) impairing DDR transcriptional activation and compromising repair potential. Acquired KDM6A loss-of-function mutations are implicated in chemoresistance, although a significant percentage of relapsed-AML has upregulated KDM6A. Olaparib treatment reduced engraftment of *KDM6A*-mutant-AML-patient-derived-xenografts, highlighting synthetic lethality using Poly-(ADP-ribose)-polymerase-(PARP)-inhibition. Crucially, a higher KDM6A expression is correlated with venetoclax tolerance. Loss of KDM6A increased mitochondrial activity, BCL2 expression, and sensitized AML cells to venetoclax. Additionally, BCL2A1 associates with venetoclax resistance, and KDM6A loss was accompanied with a downregulated BCL2A1. Corroborating these results, dual targeting of PARP and BCL2 was superior to PARP or BCL2 inhibitor monotherapy in inducing AML apoptosis, and primary AML cells carrying *KDM6A*-domain-mutations were even more sensitive to the combination. Together, our study illustrates a mechanistic rationale in support for a novel combination therapy for AML based on subtype-heterogeneity, and establishes KDM6A as a molecular regulator for determining therapeutic efficacy.

INTRODUCTION

KDM6 proteins represent a family of histone lysine demethylases that play an important role in chromatin remodeling and transcriptional regulation during multi-cellular development and tumorigenesis (1-4). KDM6A-(UTX) and KDM6B-(JMJD3) critically regulate demethylation of H3K27-methyl residues, whereas the catalytic potential of KDM6C-(UTY) is poorly understood (1, 5-7). Growing evidence suggests involvement of KDM6A in acute myeloid leukemia (AML) pathogenesis (4, 8-12). KDM6A escapes X chromosome inactivation, and *Utx*-null homozygous female mice spontaneously develop aging associated myeloid leukemia (9, 13). In addition, *KDM6A* loss-of-function mutation is implicated in conventional chemotherapy relapse in AML, indicating tumor suppressor function (8, 10, 14). KDM6A condensation, which involves a core-intrinsically-disordered-region (cIDR), has been reported to confer tumour-suppressive activity independent of Jumonji C-(JmjC)-demethylase function (14). Recent studies suggested downregulation of KDM6A expression occurs in about 46% of cytogenetically normal-karyotype and AraC-relapsed AML patients (8). However, 37% of cases exhibited upregulated KDM6A transcripts. Thus KDM6A must function in a highly contextual fashion since there are subsets of AML cases where expression is on opposite ends of a spectrum. Therefore, the cause and pathophysiological relevance of KDM6A upregulation at chemotherapy relapse, observed in more than a third of the patients, is an open question. Additionally, to what extent KDM6A expression and function are connected with AML targeted therapy is unknown.

By contrast, KDM6B predominantly plays a context-dependent oncogenic function in hematological malignancies (15, 16). KDM6B regulates transcriptional elongation, and KDM6B expression is upregulated in myelodysplastic syndromes-hematopoietic stem/progenitors (17, 18). While KDM6A acts as a tumor suppressor and is frequently mutated in T-ALL, KDM6B is essential for the initiation and maintenance of T-ALL (19, 20). However, a subgroup of T-ALL expressing TAL1 is uniquely vulnerable to KDM6A inhibition (21). Together, KDM6A and

KDM6B possess cell type-specific functions in leukemia, with KDM6 proteins and their associated signaling emerging as important focal points for developing targeted therapy. Key cellular processes impacted by KDM6 demethylases include Th-cell development, integrated-stress-response activation, and regulation of DNA double stranded break repair.

Efficient repair of DNA damage caused by genotoxic stress is important for tissue homeostasis. Tumor cells accumulate considerable levels of DNA damage and require robust DNA-damage-repair (DDR) mechanisms for survival. AML cell survival depends upon an intact DNA repair machinery, with accumulation of DNA double-stranded-breaks (DSBs) leading to apoptosis (22). DSBs are among the most lethal DNA aberrations, and are repaired through either homologous-recombination (HR) mediated repair or non-homologous-end-joining (NHEJ) (23). Targeting DNA repair pathways for cancer therapy has gained a momentum over the past few years, with poly(adenosine 5'-diphosphate-ribose)-polymerase (PARP) inhibition for HR-deficient tumors have shown promise in clinical settings (24-26). Therefore, identifying molecular regulation of DNA repair pathways important for AML cell survival is essential for developing effective combination targeted therapy.

Here we demonstrate that KDM6 demethylases play an important role in DDR gene regulation in AML opening the potential for improved molecular targeted therapies in AML through epigenetic modulation. Together, our study addresses two important clinical questions: first, PARP inhibition would be effective for KDM6A-deficient AML, and secondly, KDM6A inhibition should potentiate PARP or BCL2 blockade in distinct subtypes of AML where KDM6A expression is upregulated or even maintained above threshold level.

MATERIALS AND METHODS

Details are included in the Supplementary methods

RESULTS

KDM6 demethylases associate with DSB repair gene expression in AML

Kdm6a deficient homozygous female mice *(Utx$^{-/-}$)* spontaneously develop aging associated AML (9). To identify genes regulated by KDM6A in AML development, we re-analyzed the available RNA-seq results from *Utx$^{-/-}$* female mice presenting with AML (ERS1090539, ERS1090541, ERS1090542), compared to *Utx$^{+/+}$* control females (ERS539514, ERS539515) (9). *Utx$^{-/-}$* and MLL-AF9 negative AML splenocytes were able to propagate leukemia in secondary recipients. Deficiency of Kdm6a led to 4014 genes being downregulated and 4703 genes upregulated (FDR: 0.01; Log_2FC: > 1.5) (Supplementary dataset S1). KDM6A JmjC-demethylase function is predominantly associated with transcriptional activation (27). Gene ontology (GO) enrichment analysis of the downregulated genes (4014) in *Utx$^{-/-}$* cells revealed enrichment of several GO terms linked with DNA repair, with the most significant being the double strand break (DSB) repair (Fig. 1A). The DSB repair term included genes of both HR and NHEJ pathways (Supplementary Fig. S1A). Re-analysis of ChIP-seq results conducted in *Utx$^{+/+}$* hematopoietic cells showed a total of 1825 Kdm6a ChIP-seq occupied genes (9), which were downregulated upon Kdm6a loss. GO analysis of these 1825 genes (Supplementary dataset S2) further revealed a significant enrichment of DNA repair associated GO terms, suggesting involvement of Kdm6a demethylase in DNA repair (Supplementary Fig. S1B).

To dissect the role of KDM6 proteins in regulating DDR gene expression in AML, we generated U937 cells using *shRNA*-expressing lentivirus vectors against KDM6A or KDM6B or both (hereafter referred as KDM6 deficient cells) (Supplementary Fig. S1C). U937 cell, originally isolated from a patient with histiocytic lymphoma, has been defined as a promonocytic myeloid

leukemia cell line, capable of monocytic differentiation and has frequently been used as a model for myeloid leukemia. Additionally, U937 cells are relatively resistant to standard chemotherapy including KDM6 small molecule inhibitor GSK-J4, and therefore can serve as a relevant model to characterize targeted therapy. KDM6 knockdown led to an increase in global H3K27me3 and a decrease in H3K27ac levels, with the difference being more prominent in KDM6B knockdown and double knockdown cells (Supplementary Fig. S1D). Deficiency of KDM6A and/or KDM6B did not affect proliferation of U937 cells (Supplementary Fig. S1E). KDM6A deficient AML cell lines did not show consistent change in myeloid differentiation (Supplementary Fig. S1F). RNA-seq analysis (FDR: 0.05; Log_2FC: > 2) suggested that there was significant downregulation ($P <$ 0.05) of > 80 DDR genes upon knockdown of KDM6A alone or KDM6B alone or both (Fig. 1B). Gene Set Enrichment Analysis (GSEA) uncovered a significantly lower enrichment of DDR pathway in KDM6A deficient AML (Fig. 1C). GO term also indicated enrichment of multiple DNA repair genes, including BRCA and RAD families, in KDM6 deficient AML (Supplementary Fig. S1G). Together, these findings suggest that KDM6 proteins are associated with DDR gene regulation in AML.

DSB repair activation induces expression of KDM6 in AML

To elucidate the function of KDM6A in mediating DSB repair in AML, we first interrogated irradiation induced alteration of KDM6A in AML cells. H3K27me3 level influences DSB repair efficiency, and decrease in H3K27me3 associates with radiation dosage, with 10 Gy irradiation causing maximum decrease (28). Interestingly, a single dose of γ-radiation (10 Gy) induced a time-dependent increase in expression of KDM6A (6 out of 6 AML cell lines tested) and KDM6B (4 out of 6 lines tested) independent of pathological or molecular subtypes (Fig. 1D; Supplementary Fig. S1H). Increase in KDM6A expression was observed as early as 30 min in KG1a cells, while OCI-AML-2 and KG1a cells showed maximum induction at 4 hours after

irradiation (Fig. 1D). Low dose irradiation in AML cells did not sufficiently induce expression of KDM6A or KDM6B (Supplementary Fig. S2A). In agreement with gene expression alteration, KDM6A protein was also upregulated on radiation accompanied with a concomitant decrease in H3K27me3 (Figs. 1E-F; Supplementary Figs. S2B-C). There was no significant induction of KDM6A or KDM6B in normal $CD34^{+}CD38^{-}CD45RA^{-}$ hematopoietic stem cells (HSCs) upon genotoxic stress (Supplementary Fig. S2D). Collectively, these results indicate that γ-IR mediated DNA repair induces KDM6 demethylase expression in AML.

Deficiency of KDM6 impairs DDR gene expression and DSB repair in AML

Efficient DSB repair has been shown to promote survival of AML cells (22). To identify target genes that sensitize AML cells to genotoxic stress, we leveraged a previously reported genome-wide pooled lentiviral *shRNA* screening performed utilizing TEX cells in response to one and three rounds of 1 Gy γ-IR (Fig. 2A) (29, 30). 'Leukemia stem cell (LSC)-like' human hematopoietic cell line TEX was generated via TLS-ERG leukemia fusion oncogene expression in cord-blood derived hematopoietic stem and progenitor cells (HSPCs), which maintains functional heterogeneity, cytokine dependency, and a functional p53 pathway (31, 32). Interestingly, *KDM6A* knockdown, similar to loss of other crucial DNA repair genes, significantly impaired proliferation in two out of three clones, suggesting a radioprotective function (Figs. 2A-B). Treatment of U937 cells using γ-IR induced HR gene expression (Fig. 2C; Supplementary Fig. S2E). In contrary, induction of DDR gene and protein expression was significantly impaired in KDM6A or KDM6B deficient AML cell lines, which was accompanied with an altered cell survival and proliferation (Fig. 2C; Supplementary Figs. S2E-H). Similar results were obtained using a different *shRNA* expression construct targeting KDM6A. Ectopic expression of full length KDM6A, but not JmjC mutant, restored DDR gene expression (Supplementary Fig. S2I). Earlier we demonstrated that treatment of AML cells using a KDM6 small molecule inhibitor GSK-J4

causes a selective increase in H3K27me3 (4). KDM6A primarily plays tumor suppressor role in demethylase independent mechanisms (9, 14). However, we and others reported that KDM6 inhibition in AML cells, with intact KDM6 expression, using GSK-J4 attenuates leukemia cell survival and leukemia development (4, 12). Apart from KG1a, all cells displayed IC_{50} greater than 2 μM, a dose we used as a sub-lethal concentration for subsequent experiments (Supplementary Figs. S3A-B). Similar to KDM6 deficiency, treatment with GSK-J4 abrogated the expression of HR and NHEJ genes, highlighting KDM6 demethylase-dependent function in DDR gene regulation (Figs. 2D-E; Supplementary Figs. S3C-J). There was a substantially higher NHEJ rate compared to HR, and KDM6 inhibition compromised HR activity more than NHEJ (Supplementary Figs. S4A-B). KDM6A deficient AML cells, regardless of *TP53* mutation status, revealed an elevated double-stranded DNA break with an attenuated γH2A.X in response to genotoxic stress (Figs. 2F-G). KDM6 inhibition in U937 cells revealed a slightly elevated basal γH2A.X (Supplementary Fig. S4C). In agreement, radiation exposure induced a time-dependent increase in γH2A.X and p-ATM in vehicle treated AML cells, whereas KDM6 blockade showed an impaired γH2A.X and p-ATM induction (Supplementary Fig. S4C). In addition, there was significant transcriptional downregulation of all three MRN components, Mre11a, Rad50 and Nbn along with loss of DSB transducer Atr in *Utx*$^{-/-}$ AML cells (Supplementary Fig. S4D). Consistent with these findings, KDM6 knockdown in human AML also caused a reduced expression of MRN (Supplementary Fig. S4E). Collectively, these results underscore that KDM6 proteins play a critical role in maintaining an elevated expression of DSB recognition genes in AML cells, and KDM6 deficiency or inhibition causes an impaired DSB repair response.

KDM6A regulates chromatin accessibility and transcriptional activation at DDR loci

To understand the mechanism of KDM6A mediated DDR gene regulation, we conducted qChIP experiments. There was a significant enrichment of KDM6A at the transcription start sites (TSS) and promoter-proximal elements of BRCA and RAD family genes in AML cells (Fig. 3A; Supplementary Fig. S4F). KDM6A downregulation was associated with a concomitant increase in occupancy of H3K27me3 at these loci in both untreated and radiation treated AML cells, further indicating demethylase-dependent transcriptional regulation (Fig. 3B; Supplementary Fig. S4G). γ-IR caused a reduction in H3K27me3 at the HR promoter-proximal loci in control cells, however, a similar decrease in locus specific H3K27me3 occupancy was either absent or negligible in KDM6A deficient cells (Fig. 3B; Supplementary Fig. S4G). KDM6A has been shown to functionally interact with SWI/SNF ATP-dependent chromatin remodeling complex to regulate chromatin accessibility, and influence gene expression (1, 9, 33). We had previously conducted ChIP-seq with the SMARCC1 (BAF155) core subunit of SWI/SNF in primary AML samples (GSE108976) (11, 34). Reanalysis of genes which showed enrichment for both SMARCC1 and KDM6A revealed a substantial overlap between SMARCC1 and KDM6A targets (2785 genes; dataset S3, $P < 0.05$), with the majority of these co-occupied genes also showing enrichment of H3K27ac, while being devoid of H3K27me3 (1676 genes) (Fig. 3C; Supplementary dataset S4). These KDM6A targets that include DNA repair genes may represent potential candidates for co-regulation by KDM6A demethylase and SWI/SNF (Fig. 3D). qChIP further demonstrated that concomitant with an increase in KDM6A occupancy there was a significant enrichment of SMARCC1, CBP and H3K27ac at the TSS and promoter regions of BRCA and RAD genes in response to radiation (Fig. 3E). SMARCC1 enrichment along with CBP and H3K27ac was also observed at the promoter region of KDM6A itself (Fig. 3F), suggesting KDM6A and SWI/SNF cooperation in DDR gene regulation.

To interrogate changes in chromatin accessibility on KDM6 loss, we performed bulk ATAC-seq in KDM6A and KDM6B deficient AML cells and compared them with unaltered control cells. In concordance with transcriptional activation function of KDM6, the number of transcription factor (TF) motifs enriched in control cells that lost accessibility in KDM6 deficient cells was much higher than the number of motifs, which gained accessibility in KDM6A/B deficient AML cells (Figs. 3G-H). Motif comparison revealed greater than 90% overlap in KDM6A or KDM6B deficient cells. There was significant loss in the binding potential of TCF, CEBP, FOXO and HOXA family, which usually promote HR gene expression (Fig. 3G). Alternatively, there was increase in binding potential of IRF, PU and PRDM (Fig. 3H), which have been shown to suppress DDR and induce genomic instability. Collectively, these results indicate that changes in chromatin accessibility correlate with lower abundance of TF binding sites required for optimal DNA gene regulation. Together this may account for the observed repression of DDR gene expression in KDM6 deficient AML, thus compromising DNA repair.

KDM6A loss renders AML cells sensitive to PARP inhibition

We next assessed whether reduced KDM6 levels would sensitize AML cells to inhibition of PARP-1 signaling. Analysis of OHSU AML (n=672), containing *de novo* and relapsed AML cases with varying molecular subtypes, showed a significant inverse correlation between KDM6A and PARP-1 expression (Figs. 4A-B; Supplementary Fig. S4H). There was no major change in PARP1 expression in KDM6 deficient U937 cells (Supplementary Fig. S4I). PARP inhibition using olaparib for 72 hr decreased intracellular PAR level and induced apoptosis in AML cells (Supplementary Figs. S5A-B). In general treatment with olaparib at concentrations below IC_{50} caused a cytostatic rather than cytotoxic effect; significant cell apoptosis was observed only at higher concentrations (Supplementary Fig. S5B). Drug dose response analysis indicated that AML cells co-treated with GSK-J4 were significantly more sensitive to olaparib

compared to the controls (Fig. 4C; Supplementary Fig. S5C). Except KG1a cells, both *TP53* wild type (OCI-AML-2, OCI-AML-5, MOLM-13) and *TP53* mutated (U937, NB4) AMLs were susceptible to olaparib in response to KDM6 inhibition (Fig. 4C). Similarly, deficiency of KDM6A sensitized AML cells to PARP inhibition (Fig. 4D). Additionally, KDM6 loss caused a differential sensitivity of select AML subtypes to a conventional chemotherapeutic agent like AraC, although daunorubicin treatment did not appreciably alter AML sensitivity (Supplementary Figs. S5D-F).

Analysis of the Beat AML dataset indicated that cells with lower KDM6A expression may harbor *FLT3-ITD* mutation (Supplementary Fig. S6A). In agreement we observed that *FLT3-ITD* expressing KDM6A deficient AML cells were relatively more sensitive to olaparib compared to the controls (Supplementary Fig. S6B). To investigate olaparib sensitivity *in vivo* we transplanted control and KDM6A deficient U937 into NOD.Cg-*Prkdc*^{scid}/J (NOD.SCID) mice (Supplementary Fig. S6C). KDM6A loss alone did not affect the overall engraftment potential. In support of our prediction, compared to vehicle treated cells, olaparib administration resulted in a significant decrease in the engraftment of KDM6A deficient, but not control, AML (Fig. 4E). To further confirm, we established AML patient-derived xenograft models carrying KDM6A nonsense mutation implicated in relapse (Fig. 4F). There was a significant reduction of human $CD45^{+}CD33^{+}$ cells in the bone marrow in mice treated with olaparib compared to vehicle treated group (Fig. 4G). Together these results suggest that KDM6A loss increases sensitivity of AML cells to PARP inhibition.

Deficiency of KDM6A increases susceptibility of AML to BCL2 blockade

BCL2 inhibitor venetoclax has shown promise in the clinical setting, although a majority of the initial responders relapse (35, 36). Beat AML analysis indicated that monocytic (Mono) AML cases associate with venetoclax resistance (37), as well $KDM6A^{hi}$ expressing male AMLs are relatively more tolerant to venetoclax (Figs. 5A-B). We re-analyzed the available RNA-seq

dataset from venetoclax resistant Mono-AML ROS^{low} LSCs, and compared with venetoclax sensitive Prim-AML Ros^{low} LSCs (38). In agreement with earlier findings Mono-AML showed a relatively lower BCL2, and there was a significant increase in BCL2A1 expression in Mono-AML compared to Prim-AML (Fig. 5C; Supplementary Fig. S6D). BCL2A1 is a predictive biomarker of venetoclax resistance in AML and induces resistance to BCL2 inhibitor ABT-737 in CLL (39, 40). Consistent with these findings, the OHSU AML dataset further suggested a positive correlation between KDM6A and BCL2A1 expression (Fig. 5D). KDM6A downregulation induced BCL2, which was accompanied with a concomitant decrease in BCL2A1 gene expression (Figs. 5E-F; Supplementary Figs. S6E-G). We further reanalyzed available transcriptome dataset (FDR: 0.05; Log_2FC: > 1.25) (14) of *KDM6A*-null THP1 cells ectopically expressing full length *KDM6A* or various domain mutants of *KDM6A* (Supplementary Fig. S6H). Gain in full-length *KDM6A*, but not TPR or JmjC deletion mutants to some extent, induced BCL2A1 expression in THP1 cells (Supplementary Fig. S6I). Although cIDR-deleted *KDM6A* mutant did not restraint BCL2A1 induction, chimeric IDRs partly restored BCL2A1 expression (Supplementary Fig. S6I). In addition, qChIP analysis performed in our AML cell lines panel identified KDM6A occupancy at BCL2 or BCL2A1 TSS and promoter regions (Supplementary Figs. S6J-K). While KDM6A deficiency resulted in increased occupancy of p300 and H3K27ac at BCL2 promoter, there was increased H3K27me3 and reduced p300 at BCL2A1 loci in KDM6A deficient AML cells (Fig. 5G; Supplementary Fig. S6L). Additionally, corroborating these results GSK-J4 treatment at respective IC_{50} doses induced BCL2 expression in select AML subtypes (except MOLM-13 and Kasumi1 cells) (Fig. 5H; Supplementary Figs. S6M-N). Collectively, these findings indicate that KDM6A differentially regulates BCL2 family gene expression, and KDM6A loss correlates with BCL2 induction.

BCL2 induction commonly associates with venetoclax function (41). GSK-J4 mediated BCL2 induction in AML subtypes further prompted us to interrogate venetoclax sensitivity.

Indeed, dose response analysis revealed that *TP53* wild type (OCI-AML-2, OCI-AML-5) as well as *TP53* mutant (NB4, KG1a) AML cells co-treated with either varying doses of GSK-J4 or constant doses of GSK-J4, set at half of the IC_{50} concentrations of respective cell types, were significantly more sensitive to venetoclax compared to the monotherapies alone (Fig. 6A). Although MOLM-13 partially responded to this combination, Kasumi1 cells did not show any effect (Fig. 6A). Similarly, deficiency of KDM6A also sensitized AML cells to BCL2 inhibition (Fig. 6B). In addition, olaparib treatment resulted in an increase in mitochondrial membrane potential (MMP) in KDM6A deficient AML cells compared to control cells (Fig. 6C). Inhibition of KDM6 and PARP also resulted in an increase in MMP in AML cells (Fig. 6D). Furthermore, MV4-11 venetoclax resistant (Ven-res) cells showed a decrease in MMP and ROS level compared to venetoclax sensitive (Ven-sen) group (Supplementary Figs. S7A-D). KDM6 inhibition restored ROS in MV4-11 Ven-res cells, which was further increased in presence of olaparib (Supplementary Figs. S7C-D). Intriguingly, we provide evidence that changes in BCL2 expression and mitochondrial activity associated with KDM6A loss, may account for venetoclax tolerance in AML.

Dual inhibition of PARP and BCL2 synergizes in AML

Next we investigated whether inhibition of PARP and BCL2 would have a combination effect in controlling AML cell survival. Co-treatment of olaparib and venetoclax were superior in inhibiting AML cell viability compared to the monotherapies alone (Supplementary Fig. S7E). Combination of olaparib and venetoclax showed synergistic effects in reducing cell survival in select AML subtypes including OCI-AML-2, OCI-AML-5, KG1a, NB4 and U937 (Supplementary Fig. S7E). We did not observe drug synergism in MOLM-13, Kasumi1 and HL60 cells (Supplementary Fig. S7E). Similarly, dual inhibition of PARP and BCL2 signaling induced apoptosis in AML

(Supplementary Figs. S8A-C). Interestingly, KDM6A deficient AML cell lines were even more sensitive to the combination therapy (Supplementary Figs. S8D-E).

To further confirm, we argued that KDM6A silencing may not necessarily mimic pathologically occurring *KDM6A* mutations. Therefore, we compared drug sensitivities in primary AML samples carrying either wild type *KDM6A* or different acquired domain mutants of *KDM6A* (Fig. 7A). Corroborating our findings, olaparib and venetoclax treatment showed a stronger synergistic effect in inhibiting viability of *KDM6A*-domain mutant primary AML samples compared to *KDM6A*-wild type (WT) cases (Figs. 7B-C). Although we could not test drug efficacy in cIDR-mutant, both TPR and JmjC mutants had dramatic loss of cell viability in response to olaparib and venetoclax (Fig. 7C). *NPM1*^{mut} AML848978 only showed a marginal response to the combination (Fig. 7C). Similarly, combination of PARP and BCL2 inhibition led to an increase in apoptosis in *KDM6A* mutant primary AML cells compared to the wild type control cells (Fig. 7D; Supplementary Fig. S8F). Normal HSPCs were relatively more tolerant to olaparib (average IC_{50}: 13.56 µM compared to 0.42 µM in *KDM6A*^{mut} primary AML) and venetoclax (average IC_{50}: 11.46 µM compared to 0.18 µM in *KDM6A*^{mut} primary AML) (Supplementary Figs. S8G-H). Overall, KDM6A loss had the most profound effect by compromising DNA damage response and inducing BCL2, thus rendering AML cells sensitive to PARP and BCL2 blockade (Fig. 7E). In sum, we provide evidence and rationale supporting pre/clinical testing of the novel combination targeted therapy for human AML, and posit KDM6A as an important regulator in determining therapeutic efficacy in AML subtypes.

DISCUSSION

In this study we illustrate a mechanistic connection between KDM6 function to impaired DNA repair and BCL2 dependence in AML cell survival. Although venetoclax tolerance is primarily determined by BCL2 expression, and BCLA1 associates with resistance, molecular epi/genetic regulation of these two key proteins is unknown. We provide the first evidence in support for a central regulation integrated by KDM6A demethylase towards BCL2 and BCL2A1 expression important for AML pathogenesis. Our findings that KDM6A was an important regulator for determining efficacy of both PARP and BCL2 blockade; provide support for molecular subtype guided combination targeted therapy for AML. Venetoclax in combination with other small molecule inhibitors has shown better efficacy than venetoclax alone (35, 42). Combination therapy using venetoclax with Complex I inhibitor, MAPK pathway inhibitor or cytarabine has shown promise in pre-clinical AML models (43-45). In addition, combining KDM6 pharmacological inhibition with venetoclax has been shown to be effective in MYCN amplified neuroblastoma (46). Although BCL2 inhibition has been used in combination with hypomethylating agents, their effectiveness in synergy with PARP blockade in AML remains unexplored. In agreement with our findings an ongoing study indicates that PARP Inhibition using talazoparib can enhance anti-leukemic activity of venetoclax in preclinical human AML models [Blood (2021) 138 (Supplement 1): 1176]. Therefore, stratifying AML patients based on KDM6A mutation or expression analysis, should aid in improving therapeutic combinations.

While HR mediated DSB repair is indispensable for survival of MLL-AF9 transformed AML, most therapy-related AML have an abnormal DSB response (22, 47). KDM6 inhibition was shown to induce DNA damage in differentiating ES cells (48). Inhibition of KDM6 catalytic activity impairs HR mediated DSB repair and augments radiosensitivity in solid tumors (28, 49). Therefore, unlike the demethylase-independent, tumor suppressor function of Utx in AML development, DDR gene regulation is dependent on KDM6A demethylase function (9, 11). In

addition, we provide evidence for KDM6A and SWI/SNF cooperation in regulating DDR gene expression. Different subunits of the SWI/SNF complex have been implicated to have non-transcriptional roles in DSB repair. For example, the *BRG* bromodomain was shown to directly interact with γ-H2A.X and promote chromatin remodeling around DSBs (50). Also *ARID2* facilitates *RAD51* recruitment and HR-mediated repair (51).

Tumors deficient in BRCA genes have suppressed repair system and respond to PARP inhibition (24). However, AML patients have a low mutational burden for BRCA, and only select subtypes have been shown to have defective DDR that respond well to PARP inhibition. AML1-ETO and PML-RARα driven AML have suppressed expression of key HR associated genes, and are sensitive to olaparib, whereas MLL-AF9 harboring AML is HR proficient and insensitive to PARP inhibition (25). Only when used in combination with cytotoxic drugs like cytarabine or daunorubicin does MLL-AF9 AML respond to PARP inhibition (52, 53). Therefore, inducing a 'BRCAness' phenotype, through epigenetic modulation expands the range of AML patients, previously unresponsive to treatment, that might respond to PARP inhibitors. In accordance with this we illustrate that KDM6 attenuation in general sensitizes AML to PARP inhibition.

We also demonstrate altered chromatin accessibility in KDM6 deficient AML. The majority of these changes entailed loss in accessibility to transcription factors (TFs), like TCF and FOXM, supporting KDM6A's function as a transcriptional activator. Loss of TCF was reported to attenuate DSB repair and sensitizes colorectal cancer cells to radiotherapy (54). TCF target NEIL1, a base excision repair gene, is downregulated in KDM6A deficient cells. In addition, FOXM regulates transcription of BRIP1, which cooperates with BRCA1 to promote HR repair (55). BRIP1 expression is also downregulated in KDM6A deficient AML. HOXA9 is the mediator of resistance of MLL-AF9 leukemia to olaparib (25). It promotes transcription of key HR genes involved in DSB repair, like *MCM9*, *NABP*, *BLM*, *ATM*, *RAD51C*, *RPA1*, *BRCA1* and *BRCA2*. Importantly, among genes downregulated in KDM6A deficient cells are *NABP*, *ATM*, *BRCA1*

and *BRCA2*. Additionally, our findings indicate a putative association of olaparib sensitivity with KDM6A expression and *FLT3-ITD* mutation. *FLT3-ITD* AML occurs in about 30% of all AML patients, have a high leukemic burden, poor prognosis and routinely relapse (56). FLT3-ITD has been shown to drive increased ROS production, resulting in extensive DNA damage accumulation (57). Therefore, together with low levels of KDM6A and impaired HR, it represents a suitable target for PARP inhibition. Indeed it has been demonstrated that *FLT3-ITD* AML is highly sensitive to olaparib (58).

Loss of KDM6A expression and acquired resistance for conventional chemotherapy (8) led to the impetus to further interrogate potential synthetic lethal vulnerabilities in AML In sum, we present a molecular framework highlighting that absence of KDM6A is an important mediator of compromised DDR in different AML subtypes and determining response to PARP inhibition. Collectively, our results are in agreement with previous findings showing KDM6A tumor suppressor properties. Importantly, our findings greatly extend this field both mechanistically but also in terms of clinical relevance as it not only illustrates efficacy of PARP blockade in KDM6A deficient AML, but it also highlights *proof of concept* for epigenetic modulation guided combination targeted therapy (PARP and BCL2 blockade) in a different subtype of AML where KDM6A expression is upregulated or intact. Although bi-allelic *Utx* deficiency causes evolution to myeloid neoplasms, perhaps minimal KDM6 activity is important for survival of human AML cells similar to what observed in TET2 deficient AML (59). Transcriptional adaptation in response to genetic, epigenetic or metabolic perturbations remains a cardinal phenomenon of AML evolution. Adaptive chromatin remodelling mediated by KDM6 proteins were found to be important for persistence and drug tolerance of glioblastoma stem cells (60). Future studies should investigate to what extent KDM6 proteins cooperate with clonal hematopoiesis associated mutational burden and impinge on chromatin topology and epigenomic landscape in AML pathophysiology. KDM6 demethylases have been implicated in solid tumors, and both

PARP and BCL2 inhibitors are already being tested in cancer patients, suggesting a broader scope of application. To conclude, KDM6A emerges to be a common regulator for susceptibility of AML to both PARP and BCL2 inhibition, expanding the possibility to characterize effective combination targeted therapy for AML subtypes in pre/clinical settings.

ACKNOWLEDGMENTS

We thank Drs. Kristian Helin (Addgene# 24168), Kai Ge (Addgene# 40619), Didier Trono (Addgene# 12260, 12259), Tomasz Skorski and Steven Chan for sharing plasmid constructs and cells. We also thank Alexander Avgoustis for helping with AML specimens through Leukemia Tissue Bank at Princess Margaret Cancer Centre/University Health Network. We acknowledge Nicholas Khuu, Julissa Tsao (Princess Margaret Genomics Centre, Toronto), and Drs. Arindam Maitra, Disha Banerjee, Subrata Patra (National Genomics Core/Co-TERI, National Institute of Biomedical Genomics, Kalyani, India) for next-generation sequencing services, Princess Margaret (UHN) Animal Resources Centre, Flow Cytometry Core and CSIR-IICB Flow Cytometry, Central Instrumentation, Radiation Facility and Dr. Arunima Maiti, Tata Translational Cancer Research Center (TTCRC) for Flow Cytometry sorting facility and experimental help. We thank Dr. Nabanita Dasgupta, NRS Medical College & Hospital for providing umbilical cord blood samples. We are grateful to Dr. Craig Jordan (U Colorado) for sharing transcriptome datasets of venetoclax-resistant Mono-AML, and we appreciate his comments during the preparation of this manuscript. We also thank Drs. Stephanie Xie, Helena Boutzen, Jean Wang and other members of the Sengupta and Dick laboratories for comments and helpful discussions, and Sally Desilva, Monica Doedens for administrative assistance.

This study is supported by funding from Council for Scientific & Industrial Research (CSIR) (HCP-0008, HCP-23 and P07/MLP-AS/578), Department of Biotechnology (DBT) (BT/RLF/RE-ENTRY/06/2010), Ramalingaswami Fellowship (to A.S.), DBT (BT/PR13023/MED/31/311/2015) (to A.S.), and Department of Science & Technology (DST) (SB/SO/HS-053/2013), Govt. of India (to A.S.). A.S. was a Visiting Scientist in J.E.D. laboratory at Princess Margaret Cancer Centre, Toronto, supported by Indian Council of Medical Research (ICMR)-DHR (Short-Term) International Fellowship (INDO/FRC/452/S-11/2019-20-IHD). J.E.D. acknowledges funding from the: Princess Margaret Cancer Centre Foundation, Ontario Institute for Cancer Research (OICR) with funding from the Province of Ontario, Canadian Institutes for Health Research (Foundation: 154293, Operating Grant 130412, Operating Grant 89932, and Canada-Japan CEEHRC Teams in Epigenetics of Stem Cells 127882); International Development Research Centre, Canadian Cancer Society (703212); Terry Fox Research Institute Program Project Grant; University of Toronto's Medicine by Design initiative, which receives funding from the Canada First Research Excellence Fund; and a Canada Research Chair. M.M. acknowledges support from Israel Science Foundation (ISF 1512/14), Varda and Boaz Dotan Research Center in Hemato-Oncology, and Israel Cancer Research Fund (RCDA 14-171). L.D.B. was a recipient of CSIR-Shyama Prasad Mukherjee Fellowship. S.G., W.S., S.B., A.B. acknowledge research fellowships from CSIR and S.K.B. thanks DBT for financial support. S.S., S.S.C. and M.B., S.C. received funding from CSIR and UGC, respectively.

AUTHOR CONTRIBUTIONS

Conception, study design and interpretation: A.S. Experimental design, data acquisition, analysis and interpretation: L.D.B., S.G., S.K.B. Immunoblot analysis: W.S., S.S.C. Biochemical studies: S.B., M.B., S.S., A.B., S.C. Xenotransplantation and pharmacological studies: L.J., N.M., O.I.G., A.S. Drug sensitivity and cell survival assays: S.G., S.K.B. Drug combination index analysis: W.S., S.B. ATAC-seq, RNA-seq and computational analysis: A. Mu. RNAi screening: S.S.N.A.M., M.M. Bioinformatics analysis: L.D.B., S.G., A.G.X.Z., M.B. AML tissue banking and characterization: A.A., J.A.K., A. Mi., E.R.L., D.B., M.D.M. Manuscript writing: L.D.B., A.S. Research direction, resources, fund acquisition, manuscript editing and overall supervision: J.E.D., A.S. All authors have contributed and agreed with the final version of the manuscript.

CONFLICT OF INTERESTS

J.E.D. Celgene: Research Funding; Trillium Therapeutics/Pfizer: patents for Sirp-a targeting; Graphite Bio: SAB. M.D.M. Astellas: Consultancy. No potential conflicts of interest are disclosed by the other authors.

REFERENCES

1. Tran N, Broun A, Ge K. Lysine Demethylase KDM6A in Differentiation, Development, and Cancer. Molecular and cellular biology. 2020;40(20).

2. Yu SH, Zhu KY, Chen J, Liu XZ, Xu PF, Zhang W, et al. JMJD3 facilitates C/EBPbeta-centered transcriptional program to exert oncorepressor activity in AML. Nat Commun. 2018;9(1):3369.

3. Ohguchi H, Harada T, Sagawa M, Kikuchi S, Tai YT, Richardson PG, et al. KDM6B modulates MAPK pathway mediating multiple myeloma cell growth and survival. Leukemia. 2017;31(12):2661-9.

4. Boila LD, Chatterjee SS, Banerjee D, Sengupta A. KDM6 and KDM4 histone lysine demethylases emerge as molecular therapeutic targets in human acute myeloid leukemia. Experimental hematology. 2018;58:44-51 e7.

5. Lan F, Bayliss PE, Rinn JL, Whetstine JR, Wang JK, Chen S, et al. A histone H3 lysine 27 demethylase regulates animal posterior development. Nature. 2007;449(7163):689-94.

6. Hong S, Cho YW, Yu LR, Yu H, Veenstra TD, Ge K. Identification of JmjC domain-containing UTX and JMJD3 as histone H3 lysine 27 demethylases. Proceedings of the National Academy of Sciences of the United States of America. 2007;104(47):18439-44.

7. Sen GL, Webster DE, Barragan DI, Chang HY, Khavari PA. Control of differentiation in a self-renewing mammalian tissue by the histone demethylase JMJD3. Genes & development. 2008;22(14):1865-70.

8. Stief SM, Hanneforth AL, Weser S, Mattes R, Carlet M, Liu WH, et al. Loss of KDM6A confers drug resistance in acute myeloid leukemia. Leukemia. 2020;34(1):50-62.

9. Gozdecka M, Meduri E, Mazan M, Tzelepis K, Dudek M, Knights AJ, et al. UTX-mediated enhancer and chromatin remodeling suppresses myeloid leukemogenesis through

noncatalytic inverse regulation of ETS and GATA programs. Nature genetics. 2018;50(6):883-94.

10. Greif PA, Hartmann L, Vosberg S, Stief SM, Mattes R, Hellmann I, et al. Evolution of Cytogenetically Normal Acute Myeloid Leukemia During Therapy and Relapse: An Exome Sequencing Study of 50 Patients. Clinical cancer research : an official journal of the American Association for Cancer Research. 2018;24(7):1716-26.

11. Biswas M, Chatterjee SS, Boila LD, Chakraborty S, Banerjee D, Sengupta A. MBD3/NuRD loss participates with KDM6A program to promote DOCK5/8 expression and Rac GTPase activation in human acute myeloid leukemia. FASEB journal : official publication of the Federation of American Societies for Experimental Biology. 2019;33(4):5268-86.

12. Li Y, Zhang M, Sheng M, Zhang P, Chen Z, Xing W, et al. Therapeutic potential of GSK-J4, a histone demethylase KDM6B/JMJD3 inhibitor, for acute myeloid leukemia. J Cancer Res Clin Oncol. 2018;144(6):1065-77.

13. Sera Y, Nakata Y, Ueda T, Yamasaki N, Koide S, Kobayashi H, et al. UTX maintains functional integrity of murine hematopoietic system by globally regulating aging-associated genes. Blood. 2020.

14. Shi B, Li W, Song Y, Wang Z, Ju R, Ulman A, et al. UTX condensation underlies its tumour-suppressive activity. Nature. 2021;597(7878):726-31.

15. Wei Y, Zheng H, Bao N, Jiang S, Bueso-Ramos CE, Khoury J, et al. KDM6B overexpression activates innate immune signaling and impairs hematopoiesis in mice. Blood advances. 2018;2(19):2491-504.

16. Mallaney C, Ostrander EL, Celik H, Kramer AC, Martens A, Kothari A, et al. Kdm6b regulates context-dependent hematopoietic stem cell self-renewal and leukemogenesis. Leukemia. 2019;33(10):2506-21.

17. Wei Y, Chen R, Dimicoli S, Bueso-Ramos C, Neuberg D, Pierce S, et al. Global H3K4me3 genome mapping reveals alterations of innate immunity signaling and overexpression of JMJD3 in human myelodysplastic syndrome CD34+ cells. Leukemia. 2013;27(11):2177-86.

18. Chen S, Ma J, Wu F, Xiong LJ, Ma H, Xu W, et al. The histone H3 Lys 27 demethylase JMJD3 regulates gene expression by impacting transcriptional elongation. Genes Dev. 2012;26(12):1364-75.

19. Ntziachristos P, Tsirigos A, Welstead GG, Trimarchi T, Bakogianni S, Xu L, et al. Contrasting roles of histone 3 lysine 27 demethylases in acute lymphoblastic leukaemia. Nature. 2014;514(7523):513-7.

20. Van der Meulen J, Sanghvi V, Mavrakis K, Durinck K, Fang F, Matthijssens F, et al. The H3K27me3 demethylase UTX is a gender-specific tumor suppressor in T-cell acute lymphoblastic leukemia. Blood. 2015;125(1):13-21.

21. Benyoucef A, Palii CG, Wang C, Porter CJ, Chu A, Dai F, et al. UTX inhibition as selective epigenetic therapy against TAL1-driven T-cell acute lymphoblastic leukemia. Genes Dev. 2016;30(5):508-21.

22. Santos MA, Faryabi RB, Ergen AV, Day AM, Malhowski A, Canela A, et al. DNA-damage-induced differentiation of leukaemic cells as an anti-cancer barrier. Nature. 2014;514(7520):107-11.

23. Scully R, Panday A, Elango R, Willis NA. DNA double-strand break repair-pathway choice in somatic mammalian cells. Nat Rev Mol Cell Biol. 2019;20(11):698-714.

24. Robson M, Im SA, Senkus E, Xu B, Domchek SM, Masuda N, et al. Olaparib for Metastatic Breast Cancer in Patients with a Germline BRCA Mutation. The New England journal of medicine. 2017;377(6):523-33.

25. Esposito MT, Zhao L, Fung TK, Rane JK, Wilson A, Martin N, et al. Synthetic lethal targeting of oncogenic transcription factors in acute leukemia by PARP inhibitors. Nature medicine. 2015;21(12):1481-90.

26. Maifrede S, Le BV, Nieborowska-Skorska M, Golovine K, Sullivan-Reed K, Dunuwille WMB, et al. TET2 and DNMT3A Mutations Exert Divergent Effects on DNA Repair and Sensitivity of Leukemia Cells to PARP Inhibitors. Cancer research. 2021;81(19):5089-101.

27. Dhar SS, Lee SH, Chen K, Zhu G, Oh W, Allton K, et al. An essential role for UTX in resolution and activation of bivalent promoters. Nucleic acids research. 2016;44(8):3659-74.

28. Rath BH, Waung I, Camphausen K, Tofilon PJ. Inhibition of the Histone H3K27 Demethylase UTX Enhances Tumor Cell Radiosensitivity. Molecular cancer therapeutics. 2018;17(5):1070-8.

29. Zipin-Roitman A, Aqaqe N, Yassin M, Biechonski S, Amar M, van Delft MF, et al. SMYD2 lysine methyltransferase regulates leukemia cell growth and regeneration after genotoxic stress. Oncotarget. 2017;8(10):16712-27.

30. Aqaqe N, Yassin M, Yassin AA, Ershaid N, Katz-Even C, Zipin-Roitman A, et al. An ERG Enhancer-Based Reporter Identifies Leukemia Cells with Elevated Leukemogenic Potential Driven by ERG-USP9X Feed-Forward Regulation. Cancer research. 2019;79(15):3862-76.

31. Warner JK, Wang JC, Takenaka K, Doulatov S, McKenzie JL, Harrington L, et al. Direct evidence for cooperating genetic events in the leukemic transformation of normal human hematopoietic cells. Leukemia. 2005;19(10):1794-805.

32. McDermott SP, Eppert K, Notta F, Isaac M, Datti A, Al-Awar R, et al. A small molecule screening strategy with validation on human leukemia stem cells uncovers the therapeutic efficacy of kinetin riboside. Blood. 2012;119(5):1200-7.

591 33. Boila LD, Sengupta A. Evolving insights on histone methylome regulation in human
592 acute myeloid leukemia pathogenesis and targeted therapy. Experimental hematology.
593 2020;92:19-31.
594 34. Chatterjee SS, Biswas M, Boila LD, Banerjee D, Sengupta A. SMARCB1 Deficiency
595 Integrates Epigenetic Signals to Oncogenic Gene Expression Program Maintenance in Human
596 Acute Myeloid Leukemia. Molecular cancer research : MCR. 2018;16(5):791-804.
597 35. DiNardo CD, Pratz K, Pullarkat V, Jonas BA, Arellano M, Becker PS, et al. Venetoclax
598 combined with decitabine or azacitidine in treatment-naive, elderly patients with acute myeloid
599 leukemia. Blood. 2019;133(1):7-17.
600 36. DiNardo CD, Pratz KW, Letai A, Jonas BA, Wei AH, Thirman M, et al. Safety and
601 preliminary efficacy of venetoclax with decitabine or azacitidine in elderly patients with
602 previously untreated acute myeloid leukaemia: a non-randomised, open-label, phase 1b study.
603 Lancet Oncol. 2018;19(2):216-28.
604 37. Zeng AGX, Bansal S, Jin L, Mitchell A, Chen WC, Abbas HA, et al. A cellular hierarchy
605 framework for understanding heterogeneity and predicting drug response in acute myeloid
606 leukemia. Nature medicine. 2022;28(6):1212-23.
607 38. Pei S, Pollyea DA, Gustafson A, Stevens BM, Minhajuddin M, Fu R, et al. Monocytic
608 Subclones Confer Resistance to Venetoclax-Based Therapy in Patients with Acute Myeloid
609 Leukemia. Cancer discovery. 2020;10(4):536-51.
610 39. Bose P, Gandhi V, Konopleva M. Pathways and mechanisms of venetoclax resistance.
611 Leuk Lymphoma. 2017;58(9):1-17.
612 40. Zhang H, Nakauchi Y, Kohnke T, Stafford M, Bottomly D, Thomas R, et al. Integrated
613 analysis of patient samples identifies biomarkers for venetoclax efficacy and combination
614 strategies in acute myeloid leukemia. Nature cancer. 2020;1(8):826-39.

615 41. Punnoose EA, Leverson JD, Peale F, Boghaert ER, Belmont LD, Tan N, et al.
616 Expression Profile of BCL-2, BCL-XL, and MCL-1 Predicts Pharmacological Response to the
617 BCL-2 Selective Antagonist Venetoclax in Multiple Myeloma Models. Molecular cancer
618 therapeutics. 2016;15(5):1132-44.
619 42. Pollyea DA, Amaya M, Strati P, Konopleva MY. Venetoclax for AML: changing the
620 treatment paradigm. Blood advances. 2019;3(24):4326-35.
621 43. Panina SB, Pei J, Baran N, Konopleva M, Kirienko NV. Utilizing Synergistic Potential of
622 Mitochondria-Targeting Drugs for Leukemia Therapy. Frontiers in oncology. 2020;10:435.
623 44. Han L, Zhang Q, Dail M, Shi C, Cavazos A, Ruvolo VR, et al. Concomitant targeting of
624 BCL2 with venetoclax and MAPK signaling with cobimetinib in acute myeloid leukemia models.
625 Haematologica. 2020;105(3):697-707.
626 45. Wei AH, Strickland SA, Jr., Hou JZ, Fiedler W, Lin TL, Walter RB, et al. Venetoclax
627 Combined With Low-Dose Cytarabine for Previously Untreated Patients With Acute Myeloid
628 Leukemia: Results From a Phase Ib/II Study. J Clin Oncol. 2019;37(15):1277-84.
629 46. Lochmann TL, Powell KM, Ham J, Floros KV, Heisey DAR, Kurupi RIJ, et al. Targeted
630 inhibition of histone H3K27 demethylation is effective in high-risk neuroblastoma. Science
631 translational medicine. 2018;10(441).
632 47. Jacoby MA, De Jesus Pizarro RE, Shao J, Koboldt DC, Fulton RS, Zhou G, et al. The
633 DNA double-strand break response is abnormal in myeloblasts from patients with therapy-
634 related acute myeloid leukemia. Leukemia. 2014;28(6):1242-51.
635 48. Hofstetter C, Kampka JM, Huppertz S, Weber H, Schlosser A, Muller AM, et al. Inhibition
636 of KDM6 activity during murine ESC differentiation induces DNA damage. J Cell Sci.
637 2016;129(4):788-803.

638 49. Katagi H, Louis N, Unruh D, Sasaki T, He X, Zhang A, et al. Radiosensitization by
639 Histone H3 Demethylase Inhibition in Diffuse Intrinsic Pontine Glioma. Clinical cancer research :
640 an official journal of the American Association for Cancer Research. 2019;25(18):5572-83.
641 50. Lee HS, Park JH, Kim SJ, Kwon SJ, Kwon J. A cooperative activation loop among
642 SWI/SNF, gamma-H2AX and H3 acetylation for DNA double-strand break repair. The EMBO
643 journal. 2010;29(8):1434-45.
644 51. de Castro RO, Previato L, Goitea V, Felberg A, Guiraldelli MF, Filiberti A, et al. The
645 chromatin-remodeling subunit Baf200 promotes homology-directed DNA repair and regulates
646 distinct chromatin-remodeling complexes. The Journal of biological chemistry.
647 2017;292(20):8459-71.
648 52. Zhao L, So CWE. PARPi potentiates with current conventional therapy in MLL leukemia.
649 Cell Cycle. 2017;16(20):1861-9.
650 53. Maifrede S, Martinez E, Nieborowska-Skorska M, Di Marcantonio D, Hulse M, Le BV, et
651 al. MLL-AF9 leukemias are sensitive to PARP1 inhibitors combined with cytotoxic drugs. Blood
652 advances. 2017;1(19):1467-72.
653 54. Kendziorra E, Ahlborn K, Spitzner M, Rave-Frank M, Emons G, Gaedcke J, et al.
654 Silencing of the Wnt transcription factor TCF4 sensitizes colorectal cancer cells to (chemo-)
655 radiotherapy. Carcinogenesis. 2011;32(12):1824-31.
656 55. Monteiro LJ, Khongkow P, Kongsema M, Morris JR, Man C, Weekes D, et al. The
657 Forkhead Box M1 protein regulates BRIP1 expression and DNA damage repair in epirubicin
658 treatment. Oncogene. 2013;32(39):4634-45.
659 56. Daver N, Schlenk RF, Russell NH, Levis MJ. Targeting FLT3 mutations in AML: review
660 of current knowledge and evidence. Leukemia. 2019;33(2):299-312.

57. Sallmyr A, Fan J, Datta K, Kim KT, Grosu D, Shapiro P, et al. Internal tandem duplication of FLT3 (FLT3/ITD) induces increased ROS production, DNA damage, and misrepair: implications for poor prognosis in AML. Blood. 2008;111(6):3173-82.

58. Maifrede S, Nieborowska-Skorska M, Sullivan-Reed K, Dasgupta Y, Podszywalow-Bartnicka P, Le BV, et al. Tyrosine kinase inhibitor-induced defects in DNA repair sensitize FLT3(ITD)-positive leukemia cells to PARP1 inhibitors. Blood. 2018;132(1):67-77.

59. Guan Y, Tiwari AD, Phillips JG, Hasipek M, Grabowski DR, Pagliuca S, et al. A Therapeutic Strategy for Preferential Targeting of TET2 Mutant and TET-dioxygenase Deficient Cells in Myeloid Neoplasms. Blood cancer discovery. 2021;2(2):146-61.

60. Liau BB, Sievers C, Donohue LK, Gillespie SM, Flavahan WA, Miller TE, et al. Adaptive Chromatin Remodeling Drives Glioblastoma Stem Cell Plasticity and Drug Tolerance. Cell stem cell. 2017;20(2):233-46 e7.

675 **FIGURE LEGENDS**

676 **Figure 1 KDM6 demethylases associate with DNA repair gene expression in AML.**

677 (A) Gene Ontology (GO) term analysis of the 4014 downregulated genes in *Utx*$^{-/-}$ AML cells.

678 (B) RNA-seq heatmap showing expression of DDR genes in control and KDM6A and/or KDM6B

679 deficient U937 cells (n=5).

680 (C) Gene Set Enrichment Analysis (GSEA) for DDR pathway genes in KDM6A deficient U937

681 cells compared to control.

682 (D) Quantitative reverse transcriptase-PCR (qRT-PCR) analysis (normalized to 0h) of KDM6A in

683 AML cells treated with 10 Gy γ-irradiation (γ-IR) (n=3).

684 (E) Flow cytometry analysis showing mean fluorescence intensity (MFI) of KDM6A in OCI-AML-

685 5 cells irradiated with 10 Gy (n=3).

686 (F) Flow cytometry analysis showing MFI of H3K27me3 in OCI-AML-5 cells irradiated with 10

687 Gy (n = 3).

688 qRT-PCR values were normalized to GAPDH. Data are representative of at least three

689 independent experiments. Statistics were calculated with Student's t-test; error bars represent

690 means ± SD. **P* < 0.05 or ***P* < 0.01 were considered to be statistically significant.

691

692 **Figure 2 Loss of KDM6 in AML cells impairs DDR gene expression and double stranded**

693 **break (DSB) repair.**

694 (A) Schema representing screening assay for radiosensitive genes using pooled targeted

695 lentiviral *shRNA* library in TEX leukemia cells.

696 (B) Scatter plots showing distribution of KDM6A along with a few other known DNA repair

697 associated genes with respect to the overall gene sets analyzed in the *shRNA* screening in

698 response to 1 round *(upper panel)* or 3 rounds *(lower panel)* of radiation-recovery cycles. The

699 values on the Y-axes denote the ratio [IR (treatment)/NT (control)] of individual *shRNA*

corresponding to each gene. Analysis of clone abundance (average of four replicates) of KDM6A targeting *shRNA* clones after 1 round or 3 rounds of γ-IR (1 Gy) and recovery cycles *(right two panels)*.

(C) qRT-PCR analysis (normalized to 0h) of HR genes in control and KDM6 deficient U937 cells treated with 10 Gy of γ-IR (n=2).

(D) qRT-PCR analysis (normalized to 0h) of HR genes in DMSO (control) and GSK-J4 treated OCI-AML-2 cells treated with 10 Gy γ-IR (n=2).

(E) qRT-PCR analysis (normalized to 0h) of HR genes in DMSO and GSK-J4 treated OCI-AML-5 cells irradiated with 10 Gy (n=2).

(F) Neutral comet assay showing distance of comet tail measured in control or KDM6A deficient AML cells after 2 hr of treatment with 10 Gy of γ-IR (n=2).

(G) Immunofluorescence analysis *(left)* and quantitation *(right)* of γH2A.X foci per nucleus (n=40-50) in control or KDM6A deficient AML cells at different time points after treatment with 10 Gy of γ-IR (n=2).

qRT-PCR values were normalized to GAPDH. Data are representative of two to three independent experiments. Statistics were calculated with Student's t-test; error bars represent means ± SD. $*P < 0.05$ or $***P < 0.001$ were considered to be statistically significant.

Figure 3 KDM6A regulates chromatin architecture at DDR loci.

(A) qChIP analysis showing KDM6A chromatin occupancy on transcription start sites (TSS) of HR genes in U937 cells treated with 10 Gy of γ-IR.

(B) qChIP analysis showing H3K27me3 chromatin occupancy on TSS of HR genes in control and KDM6A deficient U937 cells treated with 10 Gy of γ-IR.

(C) ChIP-seq venn diagram analysis representing co-occupancy of KDM6A, SMARCC1 and H3K27ac (excluding H3K27me3) in primary AML.

(D) GO term analysis of the 1676 co-occupied genes from (C).

(E) qChIP analysis showing chromatin occupancy and cooperation of KDM6A and SMARCC1 (BAF155 subunit of the SWI/SNF complex) on TSS of HR genes in U937 cells treated with 10 Gy of γ-IR.

(F) qChIP analysis showing chromatin occupancy on TSS of KDM6A and KDM6B in U937 cells treated with 10 Gy of γ-IR.

(G) ATAC-seq Motif analysis, of transcription factors associated with DDR gene regulation, representing a significant loss in chromatin accessibility in KDM6A deficient U937 cells.

(H) ATAC-seq Motif analysis showing a gain in chromatin accessibility in KDM6A deficient AML.

qChIP values were normalized to IgG. Data are representative of two independent experiments. Statistics were calculated with Student's t-test; error bars represent means ± SD. $*P < 0.05$ was considered to be statistically significant.

Figure 4 KDM6A deficiency sensitizes AML to PARP inhibition.

(A) KDM6A and PARP1 mRNA expression z-scores (RNASeq v2 RSEM) heatmap cluster from OHSU AML dataset.

(B) Gene expression correlation analysis of PARP1 with KDM6A in OHSU AML cohort (n=672).

(C) Percent viability of AML cells treated with varying doses (from 1 nM to 1 mM) of GSK-J4 alone *(red)* or olaparib alone *(green)* or in combination *(blue)* for 72 hr. Data represent average of two to three independent experiments with similar results. IC_{50} values are tabulated and combination index (Ci) at ED_{50} was calculated using CompuSyn v 1.0. Ci < 1 was considered as drug synergism.

(D) IC_{50} of olaparib of control or KDM6A deficient AML cells cultured for 48 hr. Data represent average of two to three independent experiments with similar results.

(E) Bone marrow engraftment analysis of human $CD45^+$ cells in NOD.SCIDs after treatment with vehicle or olaparib (n=5 for each treatment group).

(F) Schema representing bone marrow engraftment analysis performed in *KDM6A* mutant AML patient-derived xenografts (PDX) in response to PARP inhibition.

(G) Flow cytometry contour plots *(left)* and quantitative analysis *(right)* showing engraftment of human $CD33^+CD45^+$ cells in NSG mice after being treated with vehicle or olaparib (n=10 for each treatment group).

Statistics were calculated with Student's t-test; error bars represent means ± SD. $*P < 0.05$ was considered to be statistically significant.

Figure 5 KDM6A associates with BCL2 and BCL2A1 expression.

(A) Venetoclax tolerance (AUC) based on abundance of monocytic (Mono-) AML from Beat AML (n=702).

(B) Venetoclax tolerance analysis performed between KDM6A-low and KDM6A-high expressing male AML from Beat AML cohort.

(C) RNA-seq analysis showing expression of BCL2 and BCL2A1 between primitive (Prim-) AML (n=7) and monocytic (Mono-) AML (n=5) ROS^{low} LSCs.

(D) Gene expression correlation analysis between KDM6A and BCL2A1 in OHSU AML dataset (n=672).

(E) qRT-PCR analysis of control or KDM6A deficient U937 cells. Error bars represent means ± SEM.

(F) Flow cytometry staggered histogram plots showing BCL2 expression in control or KDM6A deficient U937 cells.

(G) qChIP analysis showing chromatin occupancy at BCL2 promoter region (-0.5 Kb) in control and KDM6A deficient U937.

(H) Flow cytometry staggered histogram plots showing BCL2 expression in AML cells treated with DMSO *(blue)* or GSK-J4 *(red)* at respective IC_{50} concentrations for 48 hr.

qRT-PCR and qChIP values were normalized to GAPDH and IgG, respectively. Data represent two to three independent experiments. Statistics were calculated with Student's t-test; error bars represent means ± SD if not specified otherwise. $*P < 0.05$ or $***P < 0.001$ were considered to be statistically significant.

Figure 6 Attenuation of KDM6 increases AML susceptibility to BCL2 blockade.

(A) Percent viability of AML cells treated with varying doses (from 1 nM to 1 mM) of GSK-J4 alone *(var, black)* or venetoclax alone *(orange)* or in combination *(green)* for 72 hr. Additional combination *(blue)* line represents a constant dose of GSK-J4 *(con)* used at half of the respective IC_{50} concentrations. Data represent average of two to three independent experiments with similar results. IC_{50} values are tabulated and Ci at ED_{50} was calculated using CompuSyn v 1.0. Ci < 1 was considered as drug synergism.

(B) Percent viability of control or KDM6A deficient U937 cells treated with varying doses (from 1 nM to 1 mM) of venetoclax for 48 hr. Data represent average of two to three independent experiments with similar results.

(C) Flow cytometry histogram overlay analysis showing mitochondrial membrane potential (MMP) in control or KDM6A deficient AML cells treated with olaparib (10 μM) or DMSO for 48 hr.

(D) Flow cytometry histogram overlay analysis showing MMP in AML cells treated with DMSO *(orange)* or GSK-J4 *(blue)* or olaparib *(green)* or a combination of GSK-J4 and olaparib *(red)* at respective IC_{50} doses for 72 hr.

Figure 7 KDM6A-domain mutant primary AML cells are even more sensitive to combination of PARP and BCL2 blockade.

(A) Schema showing primary AML cells carrying different *KDM6A*-domain mutants used in our study.

(B-C) Percent viability of primary AML cells, carrying (B) wild type or (C) mutant *KDM6A*, treated with varying doses (from 1 nM to 1 mM) of olaparib alone *(green)* or venetoclax alone *(blue)* or in combination *(red)* for 48 hr. Data represent average of two independent experiments with similar results. IC_{50} values are tabulated and Ci at ED_{50} was calculated using CompuSyn v 1.0. Ci < 1 was considered as drug synergism.

(D) Flow cytometry contour analysis showing apoptotic cell populations in *KDM6A*-wild type *(upper panels)* and *KDM6A*-mutant *(lower panels)* primary AML patient-derived mononuclear cells in response to either DMSO, olaparib, venetoclax, or a combination of olaparib and venetoclax for 48 hr.

(E) Overall schema represents KDM6 deficiency induced sensitization of PARP and BCL2 blockade in AML

Figures

Figure 1

KDM6 demethylases associate with DNA repair gene expression in AML.

(A) Gene Ontology (GO) term analysis of the 4014 downregulated genes in *Utx-/-* AML cells.

(B) RNA-seq heatmap showing expression of DDR genes in control and KDM6A and/or KDM6B deficient U937 cells (n=5).

(C) Gene Set Enrichment Analysis (GSEA) for DDR pathway genes in KDM6A deficient U937 cells compared to control.

(D) Quantitative reverse transcriptase-PCR (qRT-PCR) analysis (normalized to 0h) of KDM6A in AML cells treated with 10 Gy γ-irradiation (γ-IR) (n=3).

(E) Flow cytometry analysis showing mean fluorescence intensity (MFI) of KDM6A in OCI-AML-5 cells irradiated with 10 Gy (n=3).

(F) Flow cytometry analysis showing MFI of H3K27me3 in OCI-AML-5 cells irradiated with 10 Gy (n = 3).

qRT-PCR values were normalized to GAPDH. Data are representative of at least three independent experiments. Statistics were calculated with Student's t-test; error bars represent means ± SD. *$P < 0.05$ or **$P < 0.01$ were considered to be statistically significant.

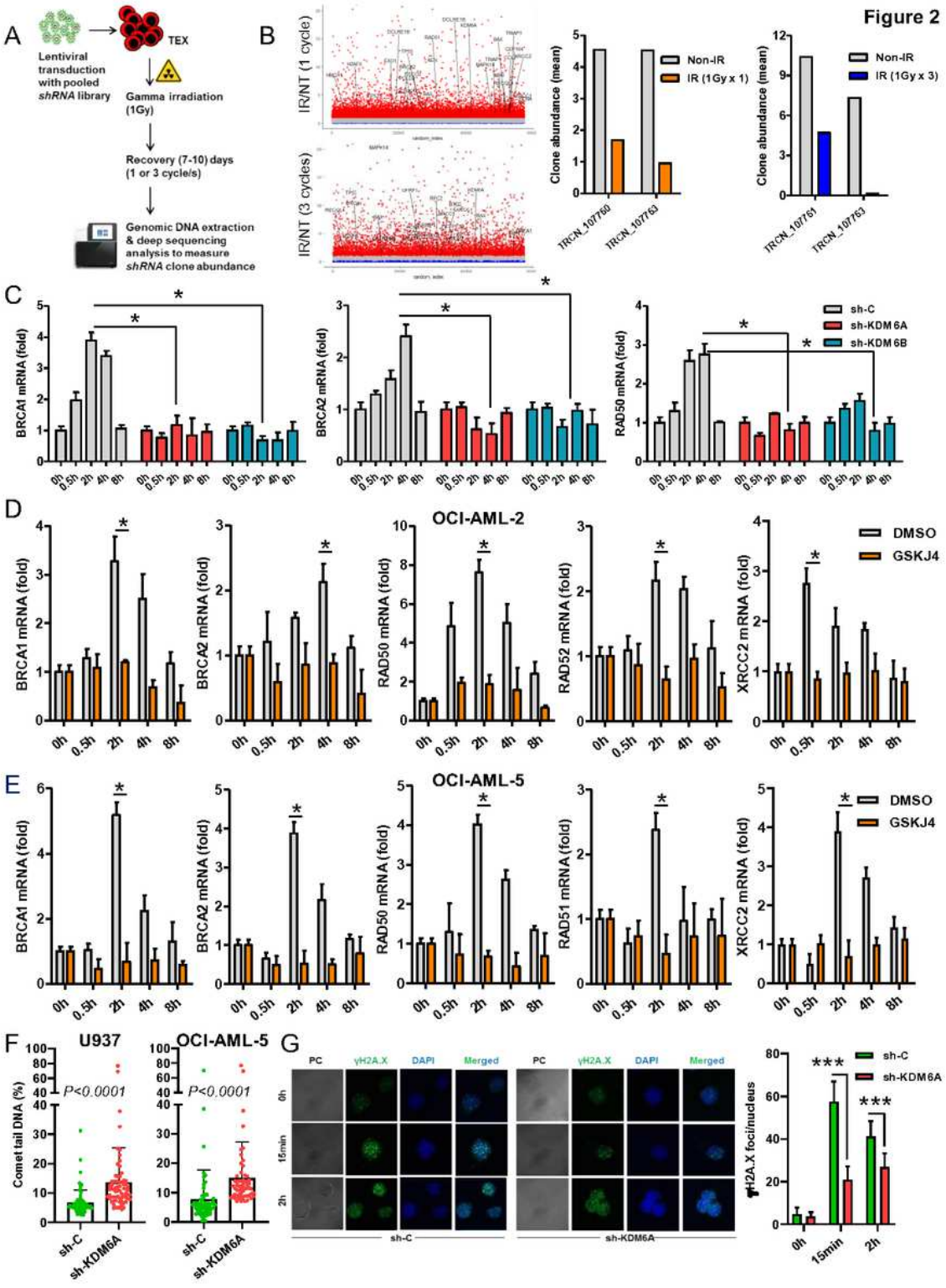

Figure 2

Loss of KDM6 in AML cells impairs DDR gene expression and double stranded **break (DSB) repair.**

(A) Schema representing screening assay for radiosensitive genes using pooled targeted lentiviral *shRNA* library in TEX leukemia cells.

(B) Scatter plots showing distribution of KDM6A along with a few other known DNA repair associated genes with respect to the overall gene sets analyzed in the *shRNA* screening in response to 1 round *(upper panel)* or 3 rounds *(lower panel)* of radiation-recovery cycles. The values on the Y-axes denote the ratio [IR (treatment)/NT (control)] of individual *shRNA*

corresponding to each gene. Analysis of clone abundance (average of four replicates) of KDM6A targeting *shRNA* clones after 1 round or 3 rounds of γ-IR (1 Gy) and recovery cycles *(right two panels)*.

(C) qRT-PCR analysis (normalized to 0h) of HR genes in control and KDM6 deficient U937 cells

treated with 10 Gy of γ-IR (n=2).

(D) qRT-PCR analysis (normalized to 0h) of HR genes in DMSO (control) and GSK-J4 treated

OCI-AML-2 cells treated with 10 Gy γ-IR (n=2).

(E) qRT-PCR analysis (normalized to 0h) of HR genes in DMSO and GSK-J4 treated OCI-AML-

5 cells irradiated with 10 Gy (n=2).

(F) Neutral comet assay showing distance of comet tail measured in control or KDM6A deficient

AML cells after 2 hr of treatment with 10 Gy of γ-IR (n=2).

(G) Immunofluorescence analysis *(left)* and quantitation *(right)* of γH2A.X foci per nucleus (n=40-50) in control or KDM6A deficient AML cells at different time points after treatment with 10 Gy of γ-IR (n=2).

qRT-PCR values were normalized to GAPDH. Data are representative of two to three independent experiments. Statistics were calculated with Student's t-test; error bars represent means ± SD. $*P < 0.05$ or $***P < 0.001$ were considered to be statistically significant.

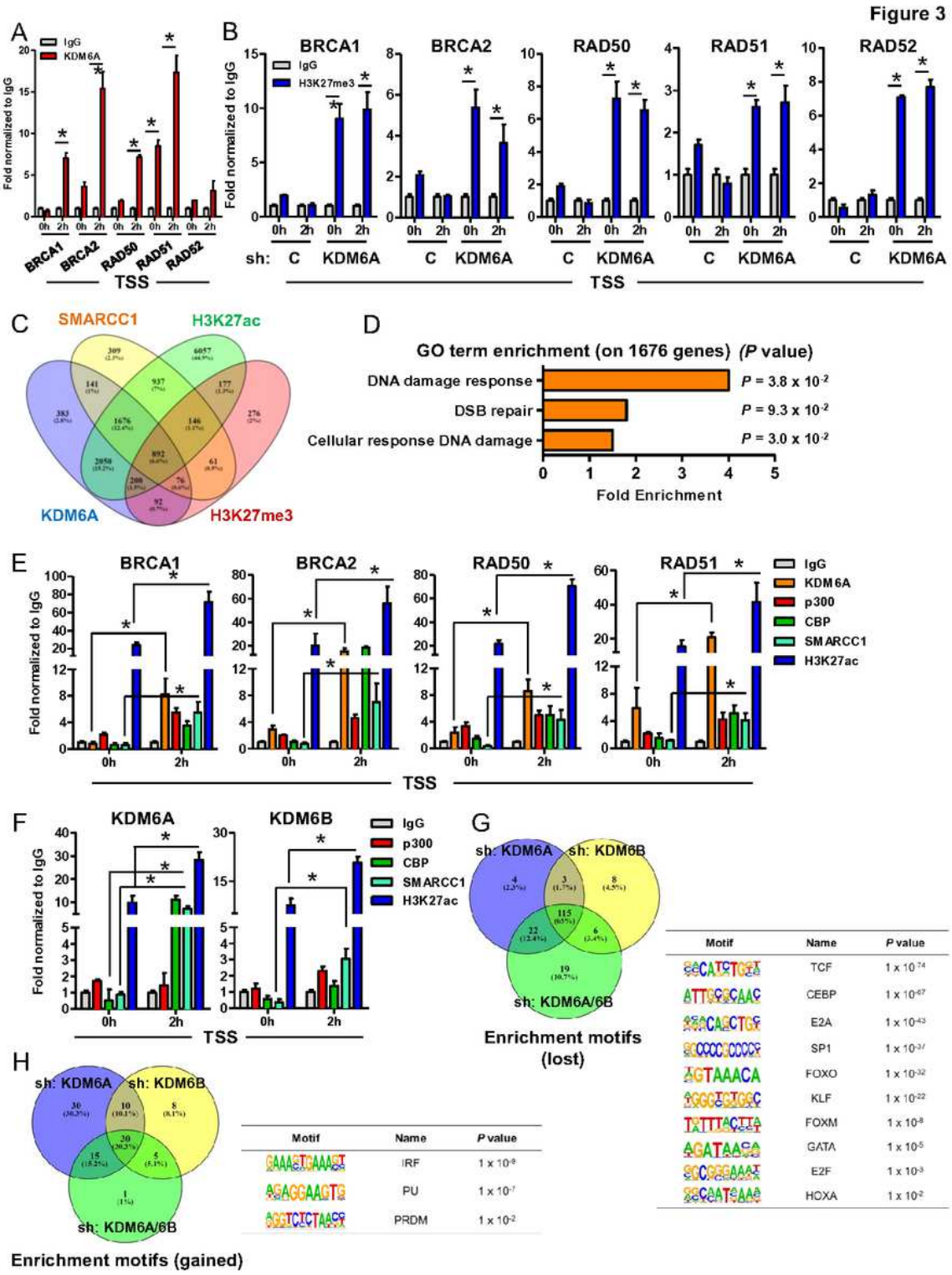

Figure 3

KDM6A regulates chromatin architecture at DDR loci.

(A) qChIP analysis showing KDM6A chromatin occupancy on transcription start sites (TSS) of HR genes in U937 cells treated with 10 Gy of γ-IR.

(B) qChIP analysis showing H3K27me3 chromatin occupancy on TSS of HR genes in control and KDM6A deficient U937 cells treated with 10 Gy of γ-IR.

(C) ChIP-seq venn diagram analysis representing co-occupancy of KDM6A, SMARCC1 and H3K27ac (excluding H3K27me3) in primary AML.

(D) GO term analysis of the 1676 co-occupied genes from (C).

(E) qChIP analysis showing chromatin occupancy and cooperation of KDM6A and SMARCC1 (BAF155 subunit of the SWI/SNF complex) on TSS of HR genes in U937 cells treated with 10 Gy of γ-IR.

(F) qChIP analysis showing chromatin occupancy on TSS of KDM6A and KDM6B in U937 cells treated with 10 Gy of γ-IR.

(G) ATAC-seq Motif analysis, of transcription factors associated with DDR gene regulation, representing a significant loss in chromatin accessibility in KDM6A deficient U937 cells.

(H) ATAC-seq Motif analysis showing a gain in chromatin accessibility in KDM6A deficient AML. qChIP values were normalized to IgG. Data are representative of two independent experiments. Statistics were calculated with Student's t-test; error bars represent means ± SD. *$P < 0.05$ was considered to be statistically significant.

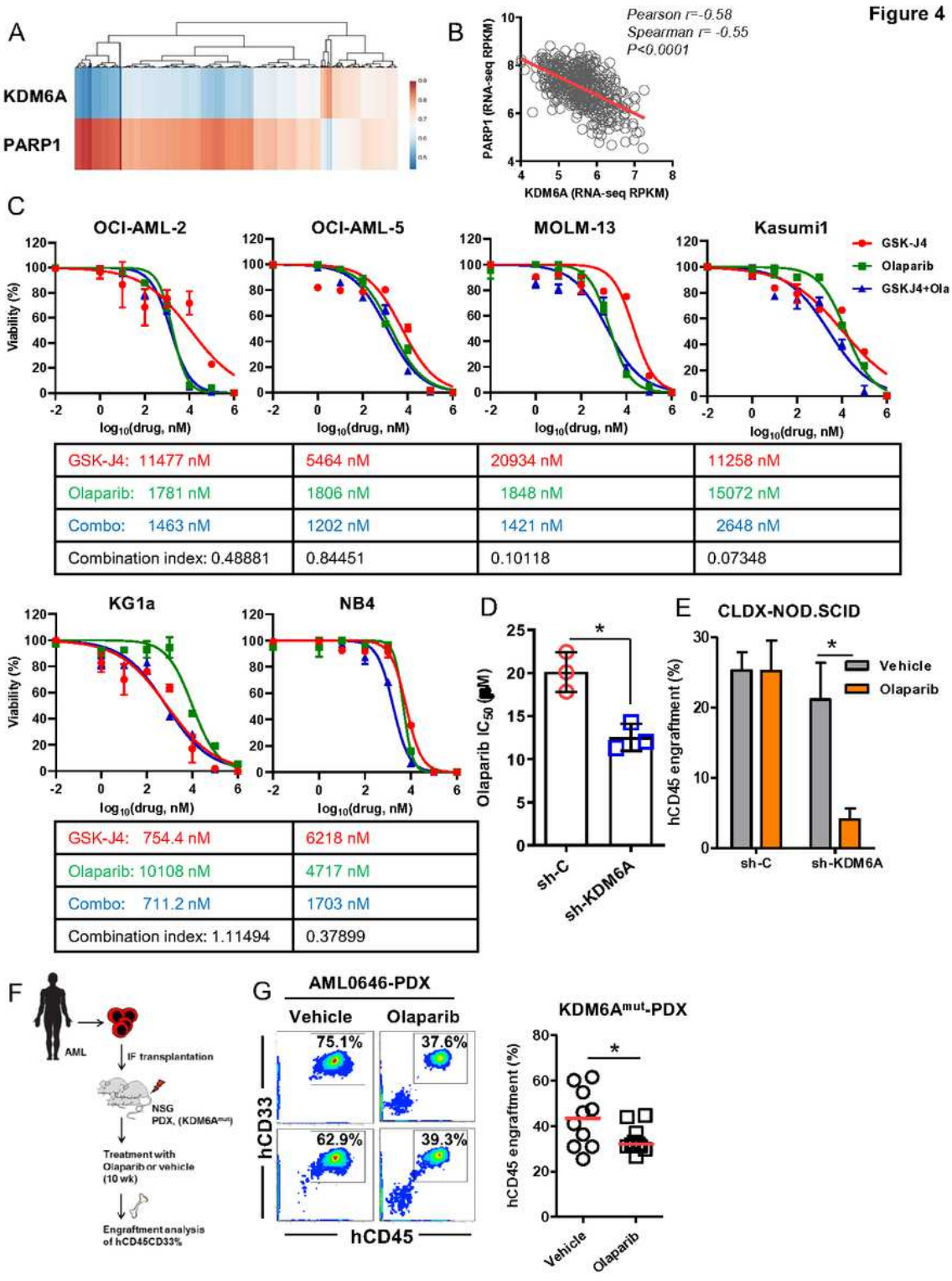

Figure 4

KDM6A deficiency sensitizes AML to PARP inhibition.

(A) KDM6A and PARP1 mRNA expression z-scores (RNASeq v2 RSEM) heatmap cluster from OHSU AML dataset.

(B) Gene expression correlation analysis of PARP1 with KDM6A in OHSU AML cohort (n=672). (C) Percent viability of AML cells treated with varying doses (from 1 nM to 1 mM) of GSK-J4 alone *(red)* or olaparib alone *(green)* or in combination *(blue)* for 72 hr. Data represent average of two to three independent experiments with similar results. IC50 values are tabulated and combination index (Ci) at ED50 was calculated using CompuSyn v 1.0. Ci < 1 was considered as drug synergism.

(D) IC50 of olaparib of control or KDM6A deficient AML cells cultured for 48 hr. Data represent

average of two to three independent experiments with similar results.

(E) Bone marrow engraftment analysis of human CD45+ cells in NOD.SCIDs after treatment

with vehicle or olaparib (n=5 for each treatment group).

(F) Schema representing bone marrow engraftment analysis performed in *KDM6A* mutant AML

patient-derived xenografts (PDX) in response to PARP inhibition.

(G) Flow cytometry contour plots *(left)* and quantitative analysis *(right)* showing engraftment of human CD33+CD45+ cells in NSG mice after being treated with vehicle or olaparib (n=10 for each treatment group).

Statistics were calculated with Student's t-test; error bars represent means ± SD. *$P < 0.05$ was

considered to be statistically significant.

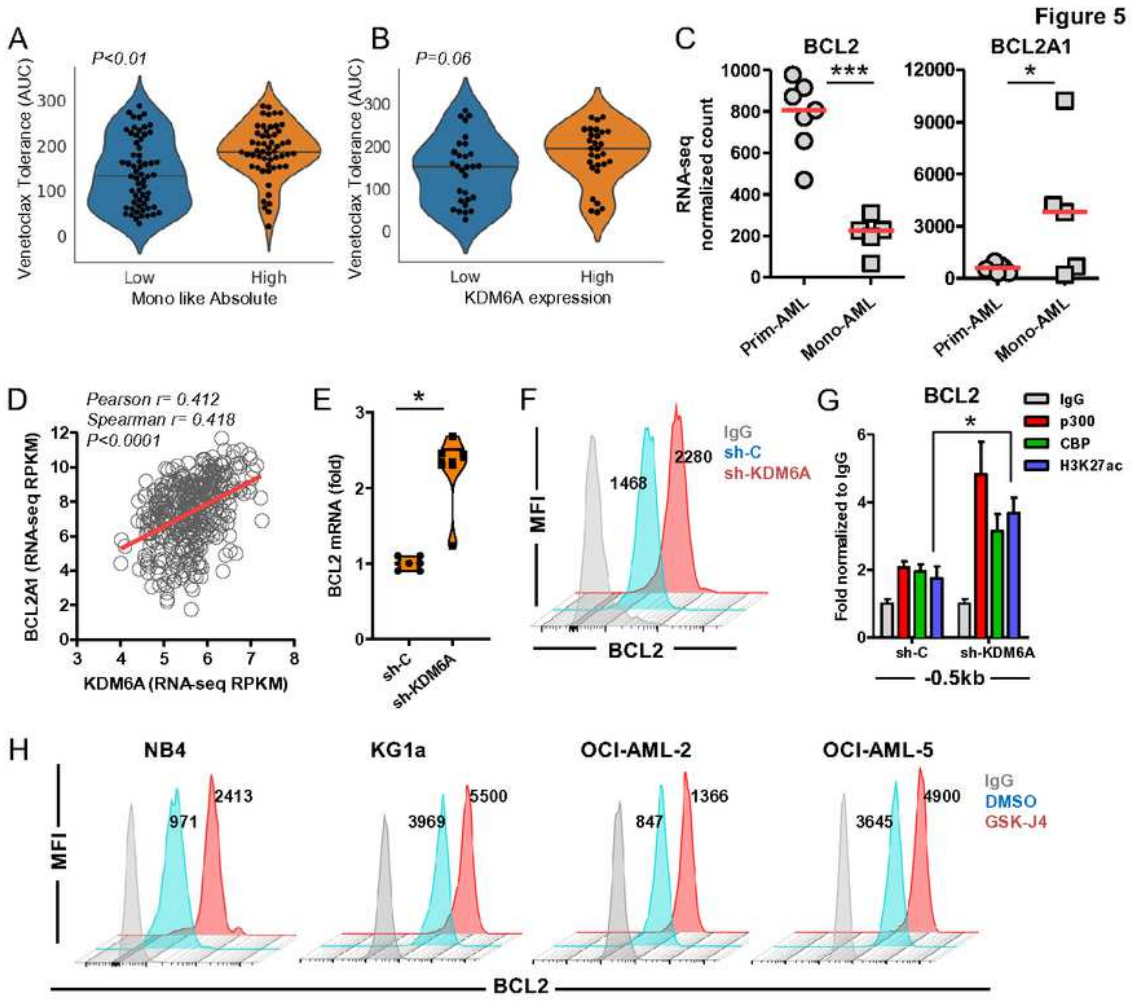

Figure 5

KDM6A associates with BCL2 and BCL2A1 expression.

(A) Venetoclax tolerance (AUC) based on abundance of monocytic (Mono-) AML from Beat

AML (n=702).

(B) Venetoclax tolerance analysis performed between KDM6A-low and KDM6A-high expressing male AML from Beat AML cohort.

(C) RNA-seq analysis showing expression of BCL2 and BCL2A1 between primitive (Prim-) AML (n=7) and monocytic (Mono-) AML (n=5) ROSlow LSCs.

(D) Gene expression correlation analysis between KDM6A and BCL2A1 in OHSU AML dataset (n=672).

(E) qRT-PCR analysis of control or KDM6A deficient U937 cells. Error bars represent means ± SEM.

(F) Flow cytometry staggered histogram plots showing BCL2 expression in control or KDM6A deficient U937 cells.

(G) qChIP analysis showing chromatin occupancy at BCL2 promoter region (-0.5 Kb) in control and KDM6A deficient U937.

(H) Flow cytometry staggered histogram plots showing BCL2 expression in AML cells treated with DMSO *(blue)* or GSK-J4 *(red)* at respective IC50 concentrations for 48 hr.

qRT-PCR and qChIP values were normalized to GAPDH and IgG, respectively. Data represent two to three independent experiments. Statistics were calculated with Student's t-test; error bars represent means ± SD if not specified otherwise. *$P < 0.05$ or ***$P < 0.001$ were considered to be statistically significant.

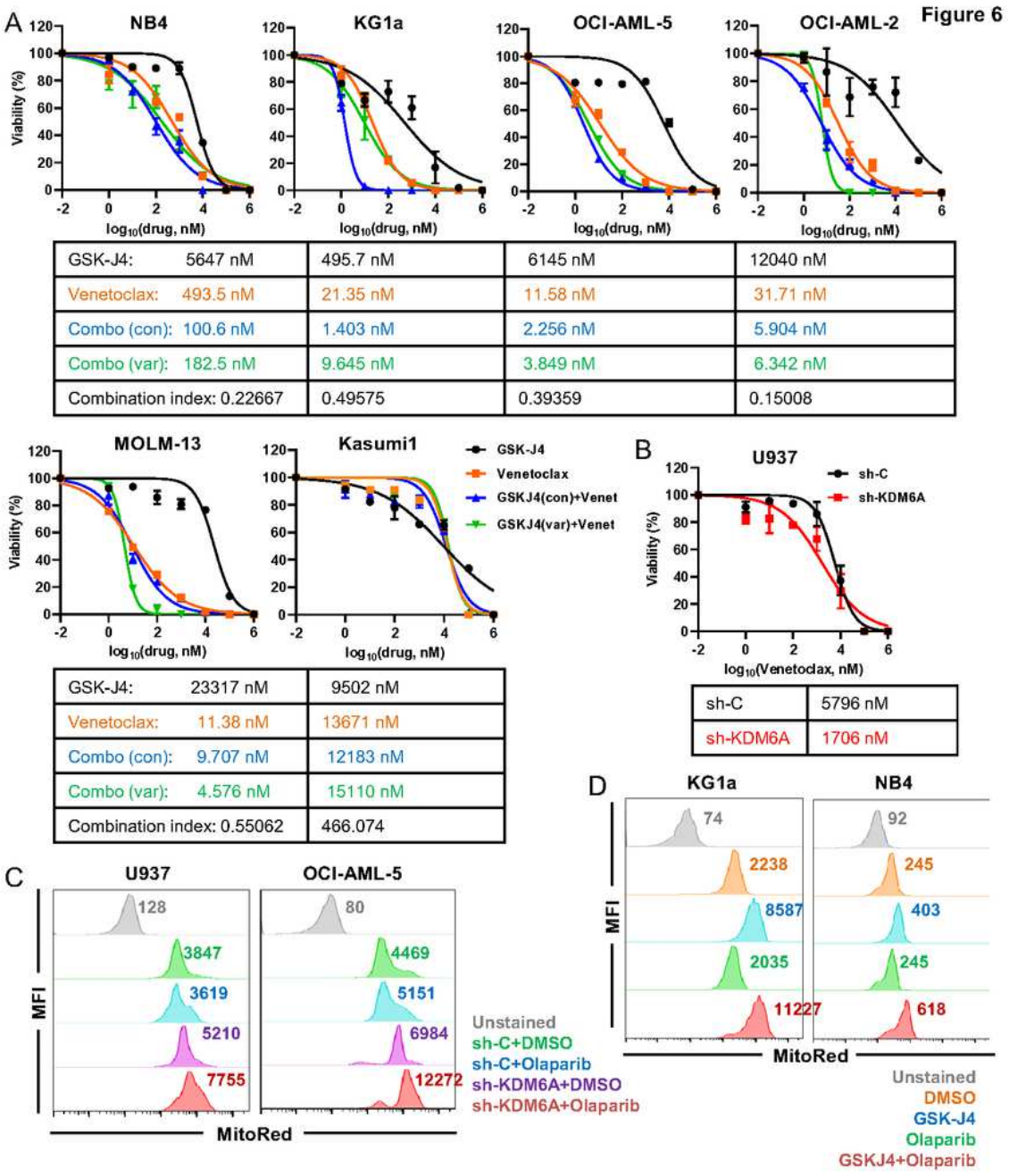

Figure 6

Attenuation of KDM6 increases AML susceptibility to BCL2 blockade.

(A) Percent viability of AML cells treated with varying doses (from 1 nM to 1 mM) of GSK-J4 alone *(var, black)* or venetoclax alone *(orange)* or in combination *(green)* for 72 hr. Additional combination *(blue)* line represents a constant dose of GSK-J4 *(con)* used at half of the respective IC50

concentrations. Data represent average of two to three independent experiments with similar results. IC50 values are tabulated and Ci at ED50 was calculated using CompuSyn v 1.0. Ci < 1 was considered as drug synergism.

(B) Percent viability of control or KDM6A deficient U937 cells treated with varying doses (from 1 nM to 1 mM) of venetoclax for 48 hr. Data represent average of two to three independent experiments with similar results.

(C) Flow cytometry histogram overlay analysis showing mitochondrial membrane potential (MMP) in control or KDM6A deficient AML cells treated with olaparib (10 μM) or DMSO for 48 hr.

(D) Flow cytometry histogram overlay analysis showing MMP in AML cells treated with DMSO *(orange)* or GSK-J4 *(blue)* or olaparib *(green)* or a combination of GSK-J4 and olaparib *(red)* at respective IC50 doses for 72 hr.

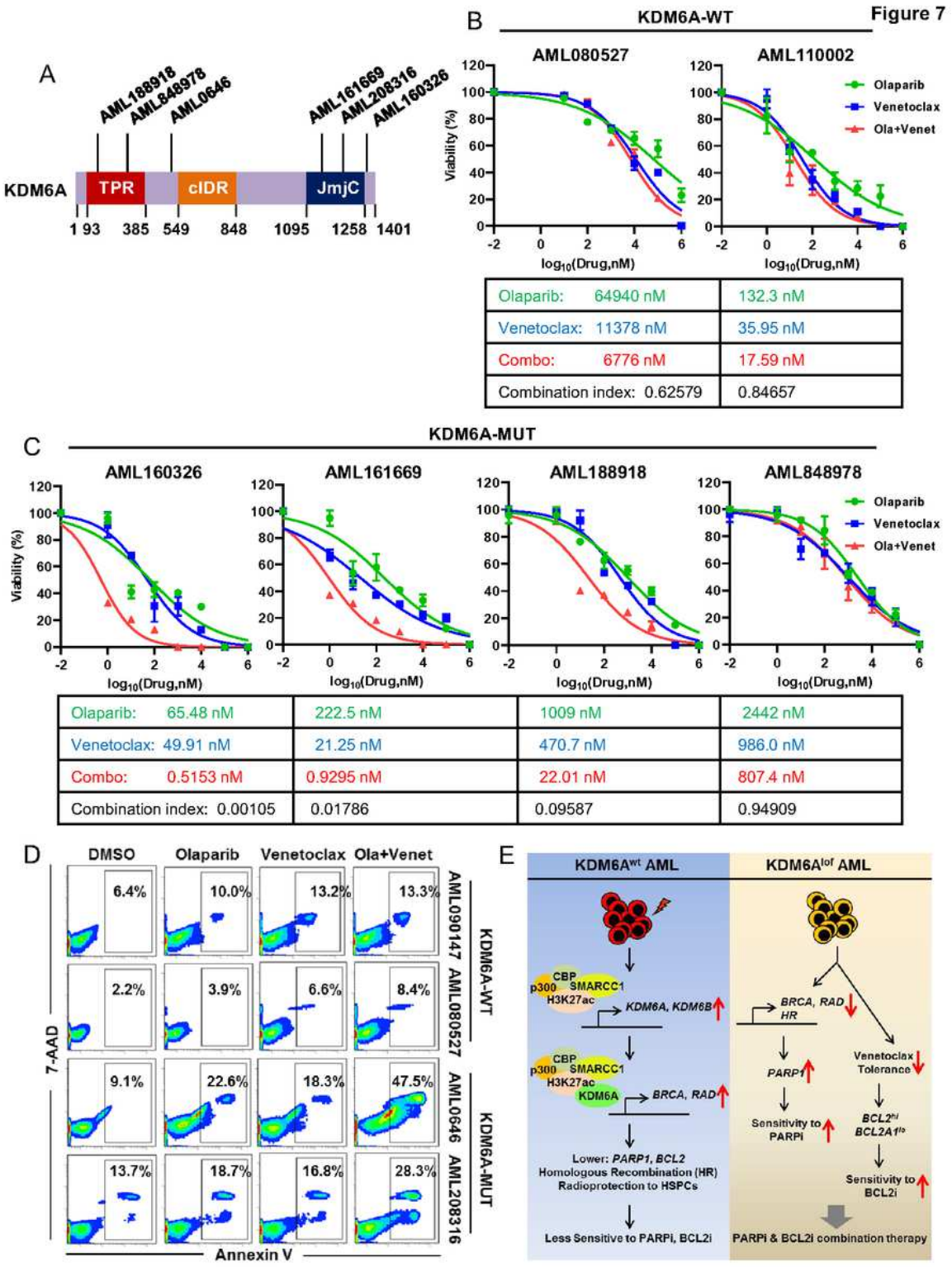

Figure 7

KDM6A-domain mutant primary AML cells are even more sensitive to **combination of PARP and BCL2 blockade.**

(A) Schema showing primary AML cells carrying different *KDM6A*-domain mutants used in our

study.

(B-C) Percent viability of primary AML cells, carrying (B) wild type or (C) mutant *KDM6A*, treated with varying doses (from 1 nM to 1 mM) of olaparib alone *(green)* or venetoclax alone *(blue)* or in combination *(red)* for 48 hr. Data represent average of two independent experiments with similar results. IC50 values are tabulated and Ci at ED50 was calculated using CompuSyn v 1.0. Ci < 1 was considered as drug synergism.

(D) Flow cytometry contour analysis showing apoptotic cell populations in *KDM6A*-wild type *(upper panels)* and *KDM6A*-mutant *(lower panels)* primary AML patient-derived mononuclear cells in response to either DMSO, olaparib, venetoclax, or a combination of olaparib and venetoclax for 48 hr.

(E) Overall schema represents KDM6 deficiency induced sensitization of PARP and BCL2

blockade in AML

Supplementary Files

This is a list of supplementary files associated with this preprint. Click to download.

- SENGUPTASupplementaryInformationCOMBINED14September2022.pdf
- debrajTable207July2022.xlsx
- SENGUPTASupplementalDataset215Apr2022.xlsx